Chapter 1

INTRODUCTION

1.1. Background

The detection of explosives in luggage has received tremendous attention due to the increasing public concern for safety and new terrorism incidents in the last few years. On July 17, 1996, TWA flight 800 exploded in the air and caused over 230 fatalities and a huge turmoil concerning the cause of the crash. The reason for the explosion was never definitely determined but one of the suspected causes was terrorism attack. This accident dramatically raised public concerns over flight and airport safety, and an increasing number of surveillance equipment is being installed at US and worldwide airports. The Federal Aviation Administration (FAA), which is responsible for airport and flight safety, has been sponsoring several projects on developing hi-tech reliable instruments for explosives detection since the 1980's, including one project at Virginia Tech. This goal of the project is to develop a prototype automatic luggage scanner for explosives detection [Conners96].

Luggage inspection using x-ray generated images is a very important and well-known technique for explosives detection [Kolla97]. However, present instruments require manual recognition of explosives and hence can be slow and labor intensive. Therefore the development of automatic luggage inspection equipment is of great importance. This thesis is a part of this project and deals with the problem of automatically detecting detonators in x-ray generated images.

Bombs favored by terrorists often consist of a charge of high explosive materials, a detonator, a timing device, a battery, and associated wiring. The detonator may contain an easily ignited low explosive, which initiates the explosion of the high explosive. The detonator type considered in this thesis is cylindrical in shape, roughly 3.63” in length and 0.16” in diameter. The goal of this research has been to develop an algorithm and software to implement automatic and accurate detection of detonators in x-ray images using object recognition techniques.

Object recognition, by definition, is the task of finding and labeling parts of an image that correspond to objects in the scene [Suetens92]. To carry out the object recognition task, we must first establish models, or general descriptions of each object to be recognized. Typically, a model includes shape, texture, and/or context knowledge about the occurrence of such objects in an image. Then the model is compared with the objects in the image using some measure to determine the similarity as well as the difference. If an object in the image is found to be similar *enough* to the model, a match is declared and the object is labeled as the model.

Object recognition has been a very important subject in computer vision [Jain95, Wechsler90] and several techniques have been developed for its implementation, among which template matching techniques have been extensively studied and developed. This thesis deals with the problem of detonator detection using template-matching methods (matched filtering and Gabor filtering) and line detection techniques with the Hough transform. Fig.1.1 shows a typical image used in this thesis. A detonator can be seen near row 150 (numbered vertically) and column 200 (numbered horizontally). The image is displayed using a Matlab image display utility, and since Matlab displays images column by column, this causes the luggage to appear to be on its side. Since the shape of a detonator is known, its detection can be considered to be a problem of locating an object with a fixed shape in an image. However, what makes this problem unique is that the detonator has an elongated shape with a very narrow width, and it must be detected in images that are often very cluttered. A detonator, when it is oriented horizontally, has a size of about 3×60 pixels in these images. However, these image dimensions may change dramatically with varying 3-dimensional (3-D) orientations, resulting in more difficulty in accurate detection. Although many researchers have considered the detection of such simple objects as lines [Ho96, Merlet96] or circular arcs [Pavlidis82], surprisingly little research has addressed the problem of detecting narrow elongated objects. The elongated shape of the detonator makes the detection problem similar to, but not equivalent to, line detection since the width of the objects is assumed to be zero in the line detection problem.

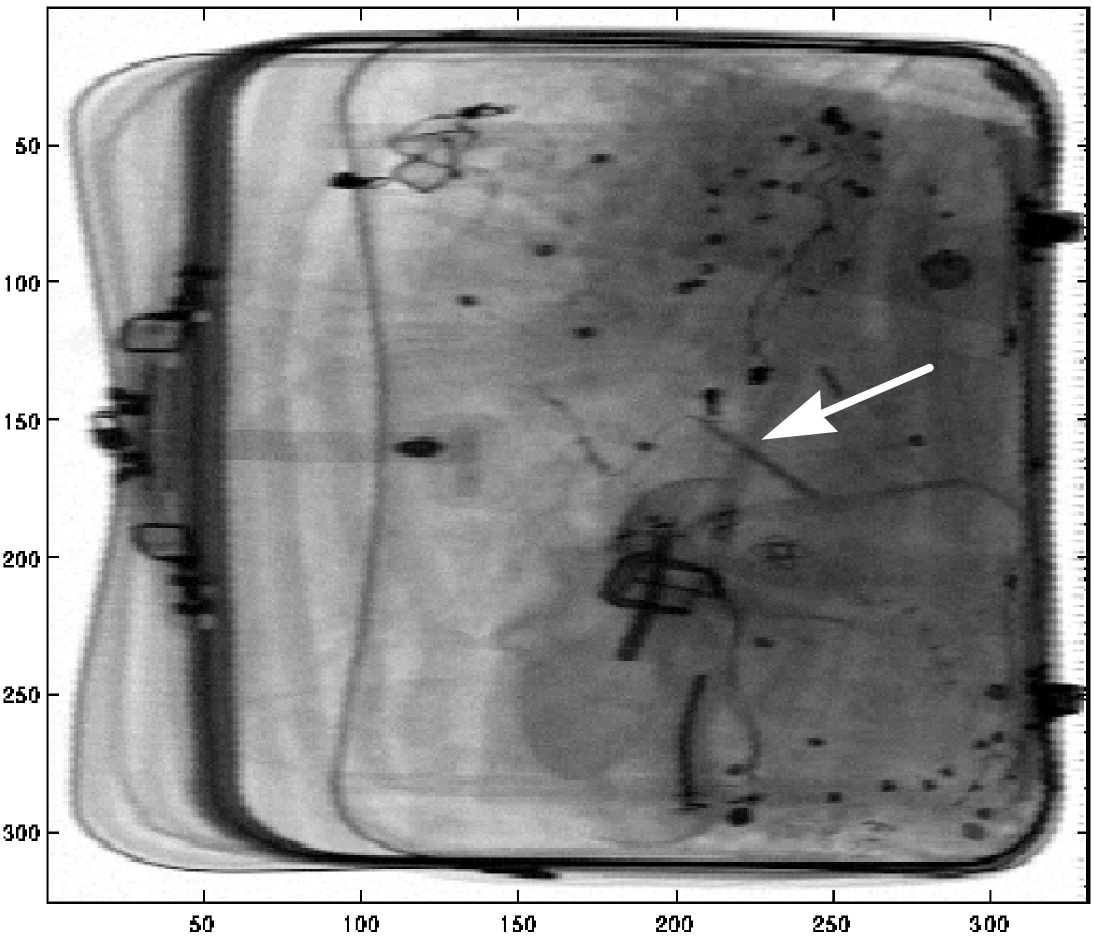

Fig. 1.1. An example of x-ray images used in this thesis. The pixels values lie in the range [0, 255], where lower numbers represent denser objects. In this image, some buttons show up as dark spots and a couple of zippers appear as darker string-like objects. The detonator is around row 150 (vertically) and column 200 (horizontally) as the arrow indicates. Matlab's display utility transposes the image rows and columns, making the luggage appear to be on its side.

1.2. Contributions of this Thesis

This thesis presents the results of part of the research project at Virginia Tech to develop a prototype hi-tech instrument for the detection of explosives using x-ray scanning. This thesis will concentrate on the detection of detonators in x-ray images. The major contribution of this thesis is that a sophisticated algorithm has been developed for detonator detection in x-ray images, and computer software utilizing this algorithm was programmed to implement the detection both on UNIX and PC platforms. This software combines matched filtering with simple geometric reasoning and information fusion. It was tested using a large number of images and was proven to be very effective even for images with different variations including overlapping, orientation changes, etc. This software provides an important step in the development of automatic equipment for explosives detection.

During the development of this software, several template matching techniques were evaluated and compared for the problem of detonator detection, and this contributes useful information on the effectiveness of these methods for the detection of line objects. A variation of matched filtering [Abbott95] was found to be reasonably effective in many cases, while Gabor filters were found not to be suitable for this detection problem. Finally, an image registration utility was developed for two different x-ray luggage scanning systems.

1.3. Organization of this Thesis

Chapter 2 describes the imaging geometry used in this thesis, and explains the mathematical relationships between a physical location in the luggage and its corresponding position in the images. In Chapter 3, the theoretical background is given for the techniques used in this thesis, including correlation-based filtering and information fusion techniques. In Chapter 4, several filters are evaluated and compared using the test images, and an algorithm is developed. Chapter 5 presents the test results of the algorithm on various images to investigate its effectiveness against image variations, such as object orientation changes, extent of overlapping, and luggage position on the conveyor, etc. An accuracy analysis of the test results will also be given. Chapter 6 presents the main conclusions drawn from this thesis. An appendix describes the image registration work between images generated on the AS&E system and those on the Fiscan system.

Chapter 2

IMAGING GEOMETRY

2.1 AS&E Geometry

Most of the images used in this thesis (except those used for Gabor filtering) were obtained on an AS&E model 101ZZ x-ray security inspection system which used the "flying spot" x-ray technology (Fig. 2.1). In this system [AS&E82], radiation generated by an x-ray tube is collimated by a long stationary slit and a rotating wheel with four slits, the combination of which causes a scanning pencil-size x-ray beam to move rapidly along a line-shaped radiation detector. The entire luggage parcel is imaged as it moves past the scanning beam on the conveyor. The detected signal is sampled, digitized, and can be either stored as an image file or displayed on a high-resolution video monitor.

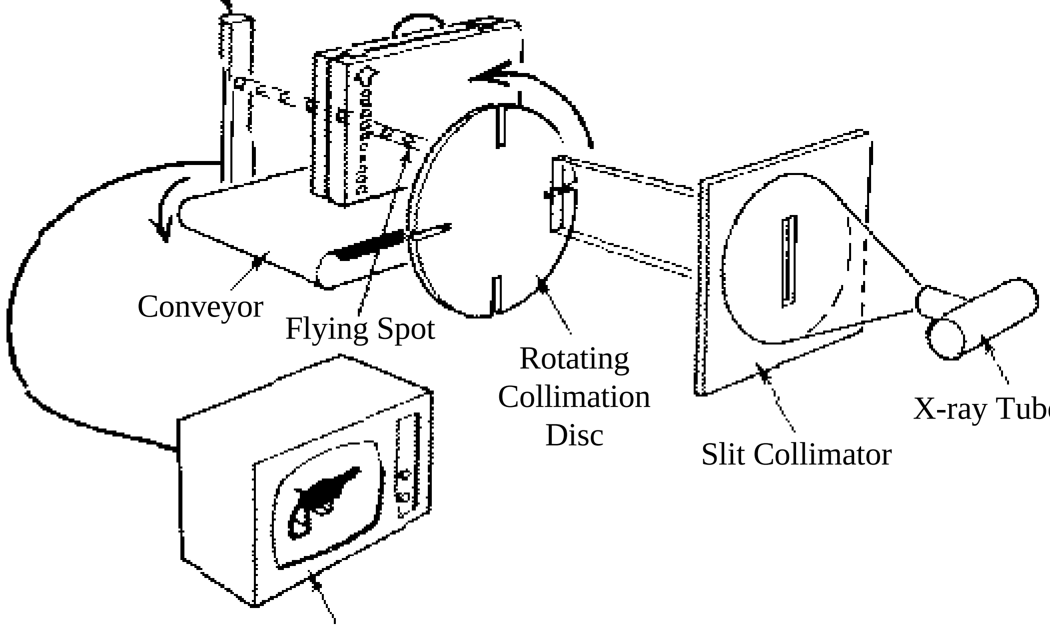

Fig. 2.1. Schematic of a AS&E x-ray inspection system [AS&E82]. Radiation generated by the x-ray tube is collimated by a stationary slit collimator and a rotating disc with four slits, the combination of which causes a scanning pencil-size x-ray beam to move rapidly along a line-shaped radiation detector. The entire luggage parcel is imaged as it moves past the scanning beam on the conveyor.

The resulting images have pixel values in the range [0, 255] (i.e., there are 8 bits per pixel), with denser objects having darker pixels. The physical dimensions of the overall image depend on the size of the luggage. To describe the orientation of the detonator, a plane perpendicular to the conveyor and to the x-ray plane that passes through the stationary slit will be used as the reference plane. In other words, the reference plane can be assumed to bisect the luggage as it travels on the conveyor. "In-plane orientation" of the detonator is defined by the angle ϕ between the principal axis of the projection of the detonator onto this plane with the direction of travel; while the "out-of-plane orientation" of the detonator is described by dihedral angle δ between the reference plane and the detonator. In this research, the image of a detonator at orientation $\phi = 40°$, $\delta = 0°$, has a size of 32×23 pixels.

In order to derive a mathematical expression for the system, Figs 2.2 and 2.3 show the cross sections of the system along and perpendicular to the x-ray path after the long stationary slit.

Referring to Fig. 2.2, it can be seen that the chopper rotates $\theta = (\frac{\pi}{2}) / N$ radians between two adjacent pixels, where N is the number of the pixels that the AS&E system samples for every image column. Let h be the total scan range of the x-ray beam as measured at the chopper wheel. The ith pixel is formed by the x-ray beam which intersects with line l at height

$$h' = \frac{h}{2} + \frac{h}{2}\tan(\theta i - \frac{\pi}{4}) \qquad (2.1)$$

Also, let l_1 be the distance of the chopper wheel from the x-ray source. From Fig. 2.3, we have

$$l_1 = h / \tan\gamma \qquad (2.2)$$

The angle γ is the angle that corresponds to the total scan range of the x-ray beam. In our system, $\gamma = 58°$.

So,

$$\tan\alpha = \frac{h'}{l_1} = \left[1 + \tan\left(\theta i - \frac{\pi}{4}\right)\right]\frac{\tan\gamma}{2} \qquad (2.3)$$

It can be seen that the relationship between h' and i is not linear, which indicates that the image quantization is not uniform in the vertical direction. This causes an image distortion along the vertical direction.

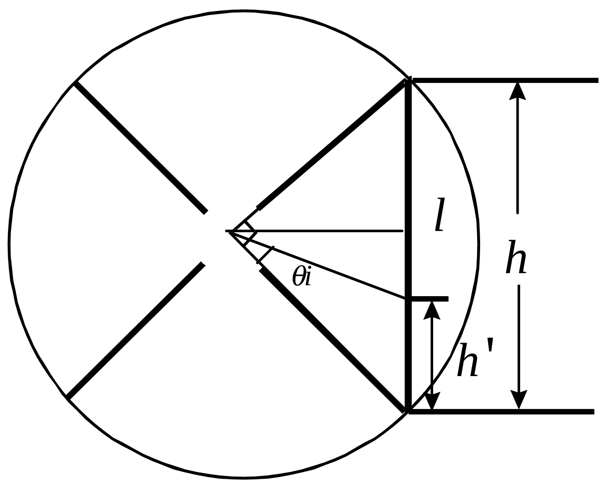

Fig. 2.2. Schematic of the rotating collimation disc (see Fig.2.1). θ is the angle that the chopper rotates between two adjacent pixels.

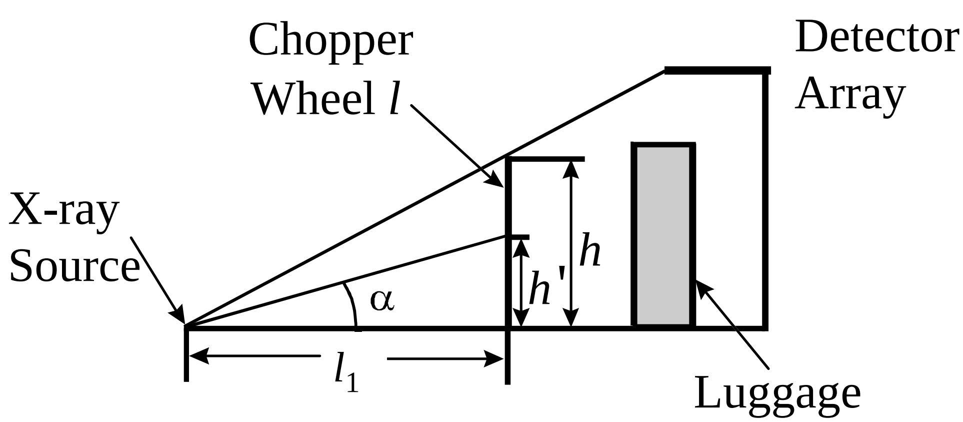

Fig. 2.3. Schematic of the system cross section along the x-ray path. As compared with Fig. 2.1, the luggage is moving away from the reader.

Two sets of images were generated to illustrate the image distortion of the AS&E system. The variations included detonator orientation and the distance between the luggage and the x-ray source. Fig. 2.4 shows an original image and the images after +10° and -10° in-plane rotation of a detonator. Although the physical angle of rotation is the same, the appearances in the images are different because of the opposite direction of rotation. In this example, an in-plane +10° rotation of the detonator causes a +8.3° angle change in the image, while an in-plane -10° rotation of the detonator results in a -4.0° angle change in the image. Fig 2.5 shows images that were obtained with the luggage at the nearest and the farthest positions of the conveyor relative to the x-ray source. The two images appear to be different, and this is because that when the luggage bag was placed at the farthest position on the conveyor, it had to be reversed to fit. The change of the position causes changes in the apparent shape and orientation of the detonator. The orientation of the detonator in the leftmost image is about 38.4°, however, in the rightmost image it is only 28.5°.

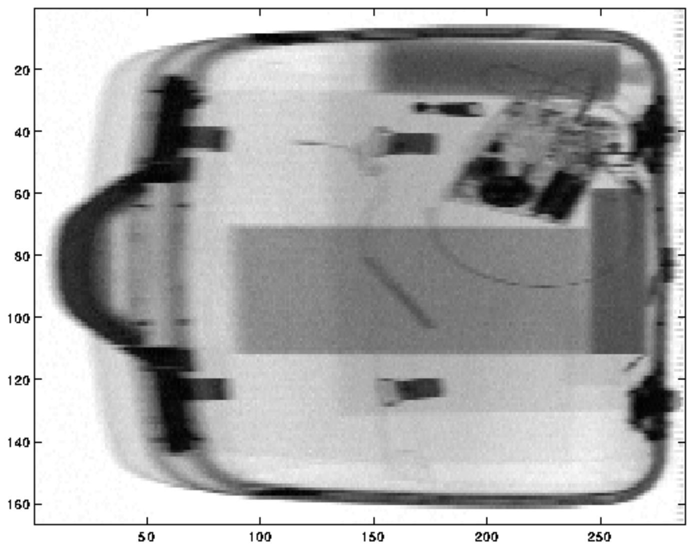
20
40
60
80
100
120
140
160
50
100
150
200
250

(a)

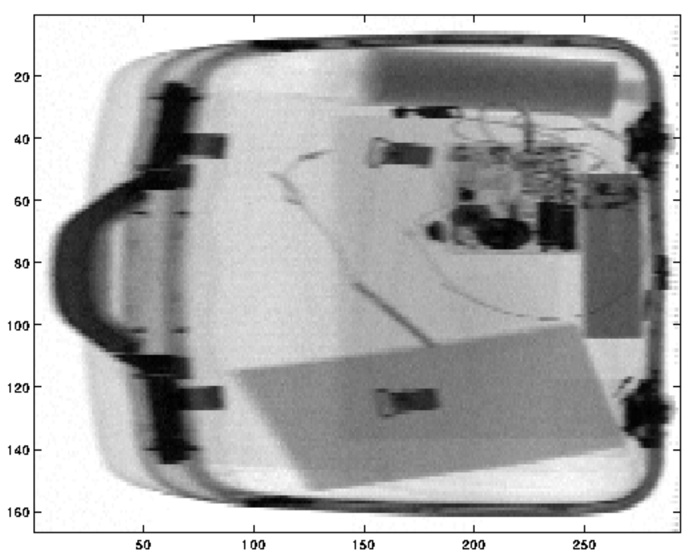
20
40
60
80
100
120
140
160
50
100
150
200
250

(b)

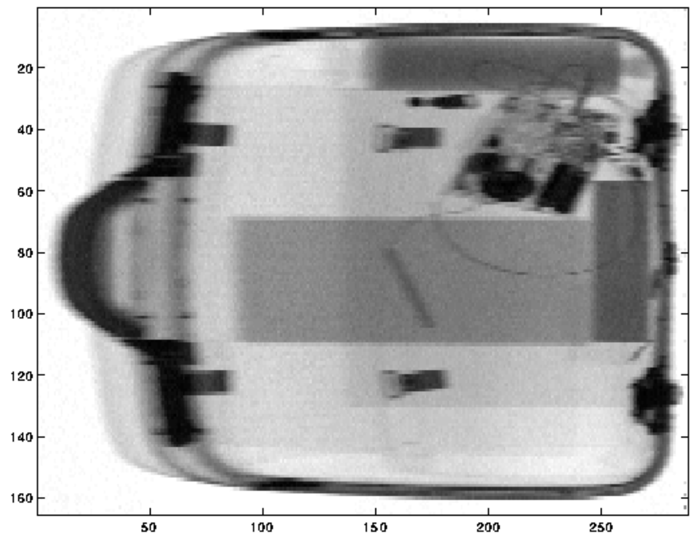

(c)

Fig. 2.4. Effect of physical rotation on the orientation of the object in the image. (a) Initial image. The detonator is around row 80 and column 150. (b) After +10° rotation. The detonator is around row 90 and column 140. (c) After -10° rotation. The detonator is around row 80 and column 150.

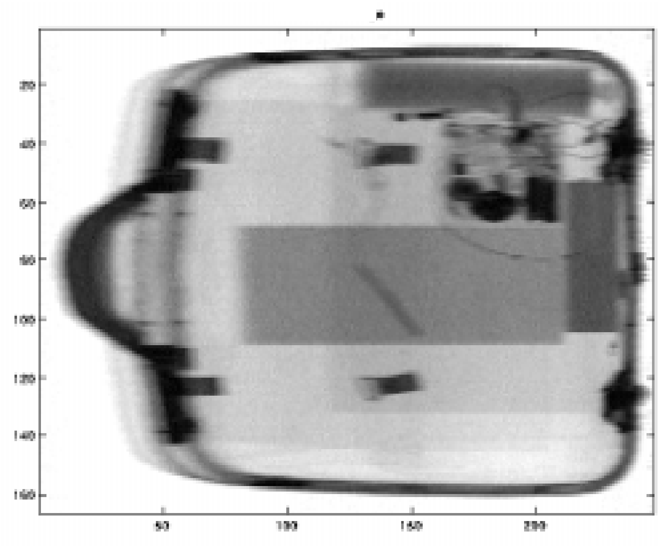

(a)

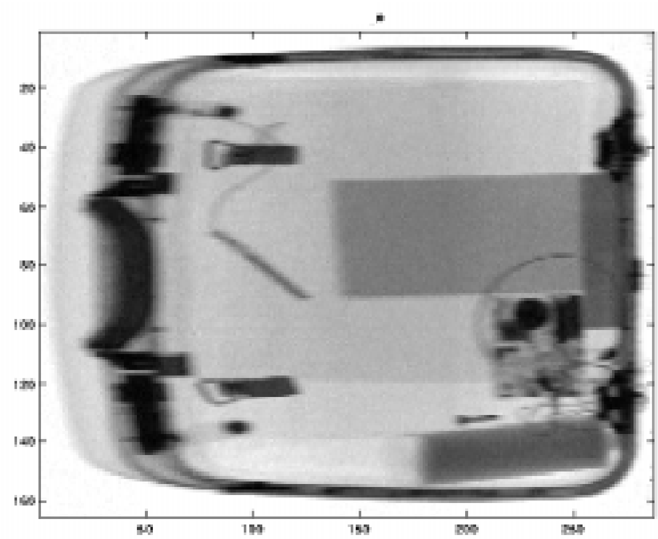

(b)

Fig. 2.5. Effect of luggage position on the conveyor on the image orientation. (a) The luggage is as far as possible from the x-ray source. The detonator is around row 80 and column 125. (b) The luggage is near the x-ray source. The detonator is now around row 70 and column 80. In obtaining these two images, the luggage contents were not changed. The reason that the two images appear different is that when the luggage bag was placed at the farthest position on the conveyor it had to be reversed to fit.

2.2 Fiscan Geometry

The x-ray images used to test a Gabor filter detection method were obtained on a Fiscan MEX-6585 x-ray inspection system. This x-ray generator generates a conical x-ray beam, which is converted to a very thin, fan-shaped beam by a lead-covered collimator [Fiscan92]. Two detector array boxes are arranged to a L-shaped line to solve the problem of corner-cutoff.

A mathematical description of the Fiscan images is given as follows:

There are total of sixteen detector boards along the L-shaped line, with eleven on the vertical line and five on horizontal line (Fig. 2.6). Let *2a* be the width of each detector board, l be the distance between the *x*-ray source and the vertical detector array, h be the height of the vertical detector array, and α_i is one half of the angle formed by the two ends of the *i*th detector board with the *x*-ray source. For the eleven vertical detector boards, we have

$$\frac{a}{\tan\alpha_{i+1}} = \frac{l}{\cos(2\alpha_1 + \cdots + 2\alpha_i + \alpha_{i+1})} \tag{2.4}$$

and for the five horizontal detector boards, we have

$$\frac{a}{\tan\alpha_{i-1}} = \frac{h}{\cos(32^\circ + 2\alpha_{16} + \cdots + 2\alpha_i + \alpha_{i-1})} \tag{2.5}$$

Consequently, $\alpha_1, \alpha_2, \cdots, \alpha_{16}$ can be determined.

Also, there are 32 pixels on each detector board. We assume that every two adjacent pixels on the same board form an equal angle corresponding to the x-ray source. Then for an arbitrary pixel *i*, we can calculate the corresponding angle formed by the pixel *i*, the *x*-ray source and the horizontal axis. For example, for pixel i on detector board k $(1 \le k \le 16)$, the corresponding angle β is:

$$\beta = 2\alpha_1 + 2\alpha_2 + \cdots + 2\alpha_{k-1} + \frac{2\alpha_k}{32}(i - 32(k-1)) . \tag{2.6}$$

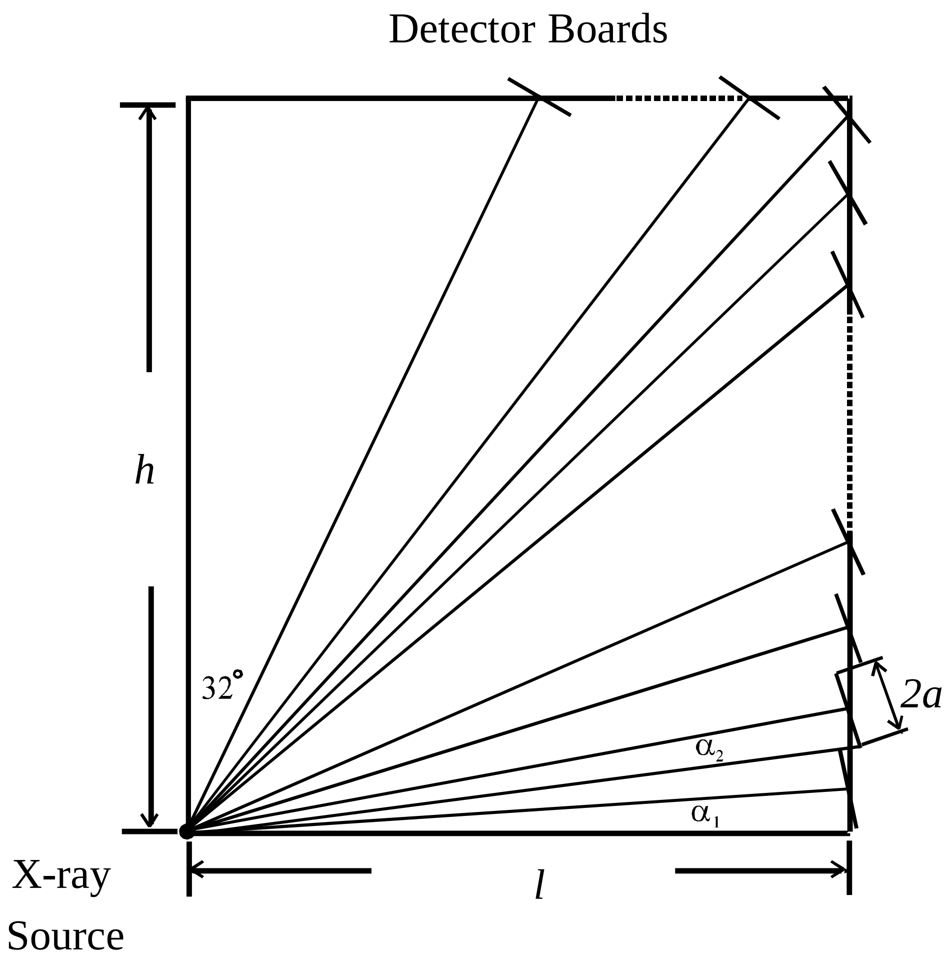

Fig. 2.6. Schematic of the Fiscan x-ray inspection system [Fiscan92]. Here *2a* is the width of the detector board, *l* is the distance between the *x*-ray source and the vertical detector array, *h* is the height of the vertical detector array, and α_i is one half of the angle formed by the two ends of the *i*th detector board with the *x*-ray source.